

A DFT study on Sumanene, Corannulene and Nanosheet as the Anodes in Li-Ion Batteries

Gharibzadeh, Fatemeh

Department of Chemistry, Tabriz Branch, Islamic Azad University, Tabriz, I.R. IRAN

Vessally, Esmail*⁺

Department of Chemistry, Payame Noor University, Tehran, I.R. IRAN

Edjlali, Ladan*⁺; Es'haghi, Moosa

Department of Chemistry, Tabriz Branch, Islamic Azad University, Tabriz, I.R. IRAN

Mohammadi, Robab

Department of Chemistry, Payame Noor University, Tehran, I.R. IRAN

ABSTRACT: *Herein, we studied interactions between the Li neutral atom and Li⁺ ion and three types of nanoparticles including sumanene (Sum), corannulene (Cor), and nanosheet to obtain the cell voltage (V) for Li-ion batteries (LIBs). Total energies, geometry optimizations, Frontier Molecular Orbital (FMO), and Density of States (DOS) analyses have been obtained using M06-2X level of theory and 6-31+G (d,p) basis set. DFT calculations clarified that the changes of energy adsorption between Li⁺ ion and nanoparticles, E_{ad} are in the order: Sheet > Sum-I > Cor > Cor-I > Sum. However, the V_{cell} for Sum is the highest. The changes in V_{cell} of Li-ion batteries (LIBs) are in the order: Sum > Sheet > Sum-i > Cor > Cor-i. This study theoretically indicates the possibility of Li as the anode in the battery field.*

KEYWORDS: *DFT study; Sumanene; Corannulene; Nanosheet; Li-ion Batteries.*

INTRODUCTION

Rechargeable batteries are very important to generation the electricity. The dry batteries, such as Zn-C, Ni-Cd, Ni-Zn and Li-ion batteries are attracted much attention because of readily transportation. Some these batteries have disadvantages including environmental issues and transportable problems [1].

Lithium (Li) is a well anode metal for rechargeable

batteries due to its low density, high specific capacity, and the lowest electrochemical potential of the periodic table [1]. One of the key points for the development of lithium-ion batteries, LIB, is to find useful electrode materials with suitable electrochemical properties. Some of the nanoparticles are suitable to use in metal-ion batteries, LIB, electronics, optics and sensor [2-8]. Recently, some efforts have been

* To whom correspondence should be addressed.

+ E-mail: l_edjlali@iaut.ac.ir ; vessally@yahoo.com
1021-9986/2020/6/51-62 12/\$/6.02

devoted to find some nanoparticles such as nanosheet and nanotube [9], dichalcogenides [10], phosphorene [11], transition metal carbides or nitrides (MXenes) [12], nanocomposites [13] in LIBs. The nanoparticles have many applications in all the chemistry field [14-19]

Our goal in this work is to theoretically study the use of some carbon nanoparticles including sumanene (Sum), corannulane (Cor) and nanosheet with different structures in LIBs as an anode. We investigated interactions between Li atom and Li⁺ ion and three nanoparticles including Sum, Cor and nanosheet (Fig. 1). Sumanene can be synthesized by oxidation of 1,5,9-trimethyltriphenylene while the first synthesis has done from norbornadiene [20]. Corannulane was first synthesized in 1966 by multistep organic synthesis [21]. The synthesis and properties of corannulane have also reported in 1971 [22].

The aim of this work is to compare the cell voltage (V) of the three nanoparticles such as Sum, Cor and nanosheet based on Li-ion battery (Table 1).

We hope that this reported computational data helps the experimental researchers to development in Li-ion battery technology.

COMPUTATION METHODS

Total energies, geometry optimizations, Frontier Molecular Orbital (FMO) and Density of States (DOS) analyses for Sum, Cor and nanosheet were calculated at the M06-2X level of theory using 6-31+G (d,p) basis set [23]. All calculations were performed in the G09 program [24]. During optimization process, all the atoms were optimized and the atoms were not fixed. The vibrational frequencies were calculated for our systems. All the structures are true minima on the potential energy surface and imaginary frequency was not obtained.

The chemical formulas of the studied nanoparticles are Sum, C₂₁H₁₂; Cor, C₂₀H₁₀; and nanosheet, C₅₄H₁₈. Hydrogen atoms are used to cap the boundary carbon atoms of the nanoparticles. The natural bond orbitals (NBO) of the Li⁺/Li-nanocone complex were calculated for charge and hybridization analysis.

The Li and Li⁺ adsorption energy is calculated by the following equation:

$$E_{\text{ad}} = E_{\text{complex}} - E_{\text{nanoparticle}} - E_{\text{Li/Li}^+} + E_{\text{BSSE}} \quad (1)$$

Where, $E_{\text{nanoparticle}}$ is the energy of the nanoparticles including Sum, Cor and nanosheet. The E_{complex} is the

energy of each nanoparticle which Li or Li⁺ adsorbed on the surface. The E_{BSSE} relates to the basis set superposition error which is calculated by the counterpoise method of *Boys* and *Bernardi* [25].

The HOMO-LUMO energy gap (E_g) is calculated as:

$$E_g = E_{\text{LUMO}} - E_{\text{HOMO}} \quad (2)$$

Where E_{LUMO} and E_{HOMO} are energies of HOMO and LUMO levels. The change of E_g is computed as follows:

$$\Delta E_g = \left[\frac{(E_{g2} - E_{g1})}{E_{g1}} \right] \times 100 \quad (3)$$

Where, E_{g1} and E_{g2} are for nanoparticles value and the complex value. This parameter indicates the electronic sensitivity of the nanoparticle to the Li/Li⁺ adsorption. The GaussSum program has been applied to calculate the DOS plots [26].

To improve the results, Sum and Cor were calculated using 6-31++G (d,p) basis set and in presence of the ethylene carbonate, EC, solvent as a battery electrolyte.

RESULTS AND DISCUSSIONS

Three types of nanoparticles were first selected to study their physical parameters and their interaction with Li neutral atom and Li⁺ ion. Then, the cell voltage (V) of the three nanoparticles based Li-ion battery (LIBs) was calculated and discussed. We examine all regions at top of pentagon or hexagon ring for possible interaction with Li neutral atom and Li⁺ ion. The global minima for interaction between Li and nanoparticles were obtained in where the Li located in middle top of the pentagon or hexagon rings.

In the case of the Sum and Cor adsorption may occur on concave or convex surfaces (Figs. 2, 5, 7 and 9). It would be important and interesting to compare the calculated data for both cases. The interaction between Li⁺ and Sum in concave surface is more (-2.35 kcal/mol) than convex surface. The interaction between Li⁺ and Cor in concave surface is slightly more (-0.42 kcal/mol) than convex surface.

Adsorption of Li/Li⁺ over the sumanene

Sumanene has benzyl positions which are active for possible organic reactions. The core of Sum is a benzene ring and the borderline consists of cyclopentadiene and benzene rings which is shown in Fig. 1. [27]. Sum has a bowl-shaped with a bowl depth of 1.18 angstrom [27].

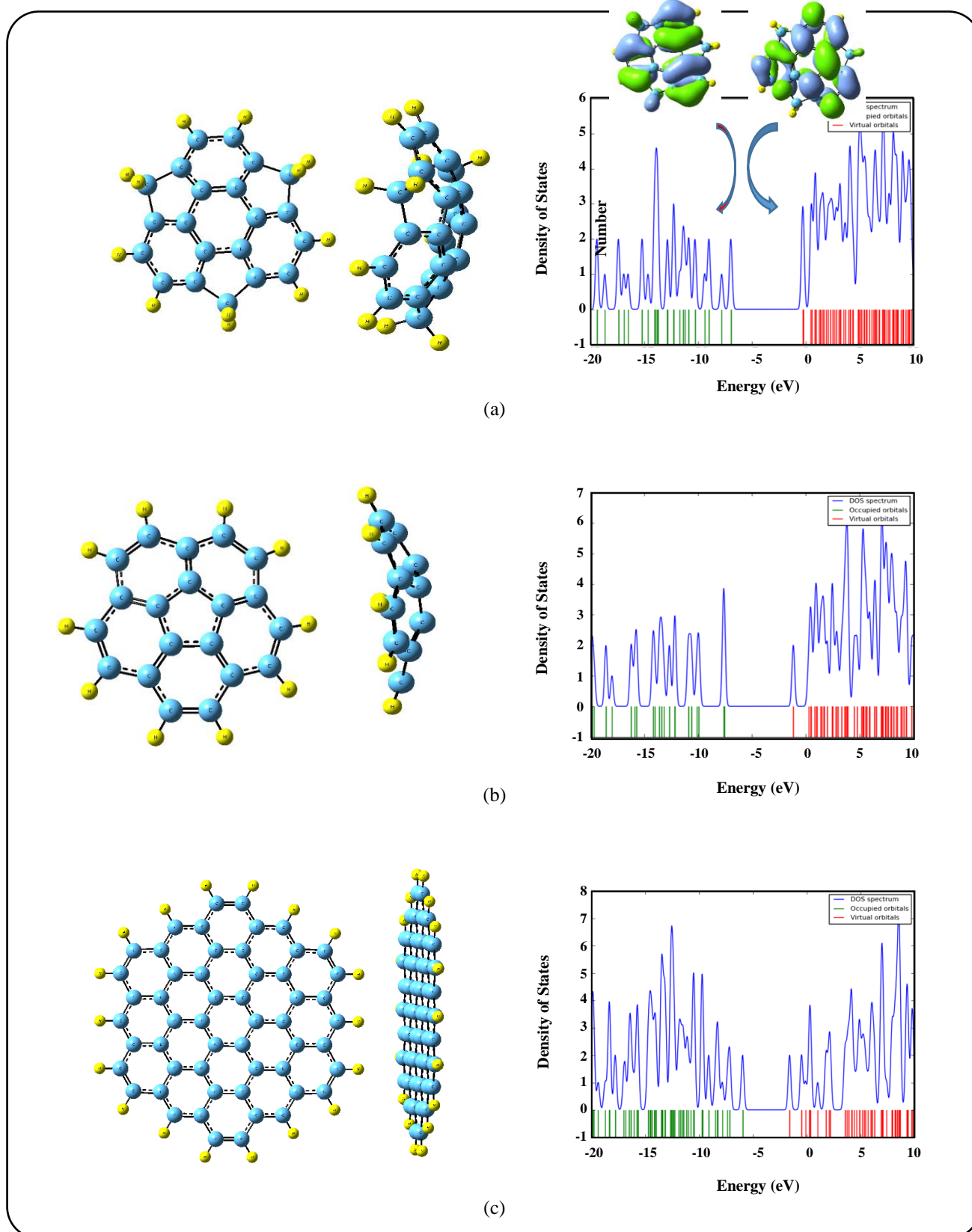


Fig. 1: Optimized molecular structures of (a) sumanene (Sum) (b) corannulene (Cor); (c) nanosheet.

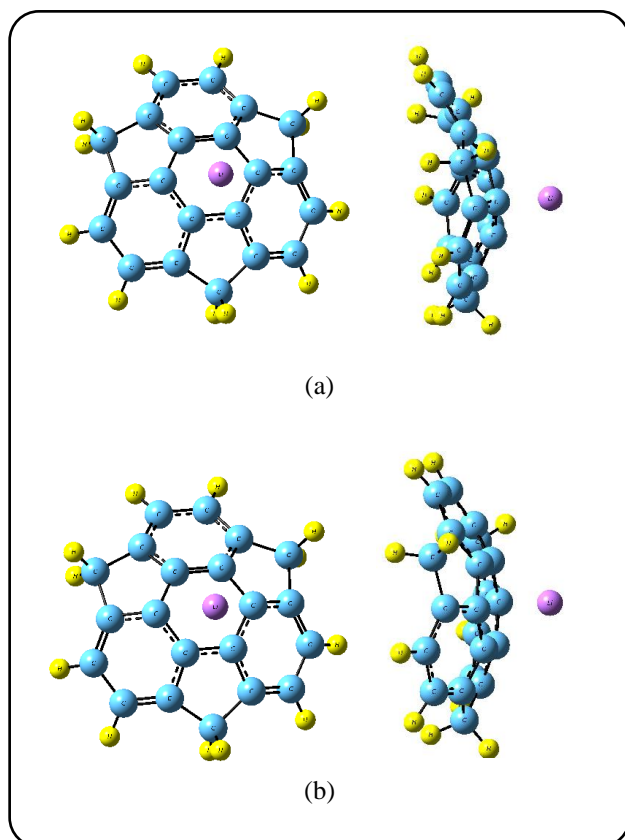


Fig. 2: Optimized structures of Li^+ and Li -Sum complexes. (a) Li^+ -Sum complex (b) Li -Sum complex. Distances are in Å.

The six hub carbon atoms are pyramidalized by 9° and Sum shows bond lengths from 1.38 to 1.43 angstrom).

The HOMO and LUMO energies are -6.95 and -0.29 eV, respectively; thus the HOMO-LUMO gap energy is 6.67 eV (Table 1). In order to study the behavior of adsorption of Li^+/Li on Sum, we must examine all possibilities of the interaction between Li^+/Li and both inside or outside the bowl.

Adsorption of Li/Li^+ outside the bowl of sumanene

During optimization, the Li^+ ion and Li atom were located above the plane of the six-membered ring of Sum with distances of 1.92 and 1.83 Å, respectively (Fig. 2). This indicates a good interaction between Sum and both Li^+ ion and Li neutral. The adsorption energy, E_{ad} , of the Li^+ ion on the Sum is -42.20 kcal mol $^{-1}$ that is larger than that of the Li neutral (-3.53 kcal mol $^{-1}$) (Table 1). Higher interaction between Sum and Li^+ ion attributed to an interaction between Lewis base and Lewis acid.

Both the HOMO and LUMO levels shift to the lower energies (more negative) for the Sum- Li^+ complex (Fig. 3).

The HOMO and LUMO levels stabilized during Li^+ adsorption so that the stabilization is sharp for LUMO level. The LUMO level considerably stabilized from -0.29 eV in Sum to -4.34 eV in the Sum- Li^+ complex (Table 1), leading to slightly decrease in the E_g ($\sim -5.6\%$). The changes in HOMO, LUMO and E_g are demonstrated in Fig. 3 by density of state (DOS) diagrams. Plot of partial density of states, PDOS, clearly indicates that a new level produced at the E_g gap of pristine mostly arises from Li^+ cation which leads to decrease slightly in E_g of the Li^+ -Sum complex (Fig. 4).

The effect of atomic Li adsorption on the electronic properties of Sum- Li is different from that of Sum- Li^+ . Unlike to the Li^+ adsorption, the Li adsorption considerably makes the SOMO unstable due to being an unpaired electron in HOMO of the Sum- Li complex. This SOMO level is changed from -6.95 to -3.55 eV which is singly occupied. In a good agreement with the sharp energy change, the shape of HOMO is changed significantly by transferring to the adsorbing area. The energy of the LUMO level is almost slightly changed from -0.29 to -0.83 eV as shown in Table 1 and Fig. 4. As a result of large change in HOMO, the E_g (2.73 eV.) is significantly narrowed by about 59.0% , indicating that the effect of Li adsorption on the E_g is much more than that of the Li^+ adsorption process. Plot of partial density of states, PDOS, (Fig. 4) clearly indicates that a new level produced at the E_g gap of pristine mostly arises from the Li neutral which leads to decrease significantly in E_g of Li -Sum complex.

The hybridization of carbon atoms in the six-membered ring in the center of the Sum is $\text{sp}^{2.1}$. After the adsorption of Li^+ , the hybridization of carbon atoms changes to $\text{sp}^{2.2}$. The DFT calculations clarified that the p character of carbon atoms in the six-membered ring increases with adsorption of Li^+ because those carbon atoms like to interact with the Li^+ cation. Strong interaction between carbon atoms in the six-membered ring and Li^+ leads to an increase of the p character of carbon atoms and consequently to an increase of the bond length from 1.44 in pristine to 1.45 Å in Li^+ -Sum complex.

Adsorption of Li/Li^+ inside the bowl of sumanene

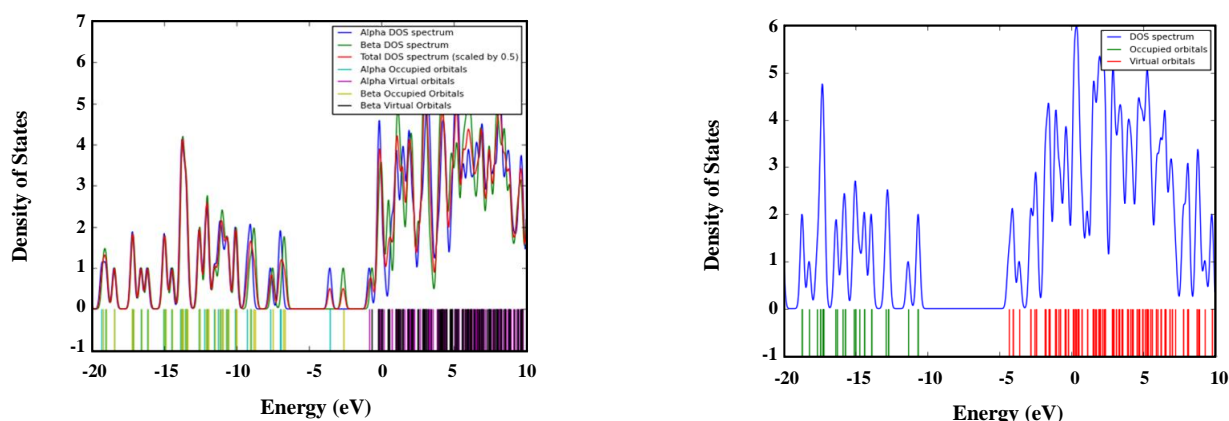
The Li^+ ion and Li atom optimized inside the plane of the six-membered ring of Sum-i with distances of 1.90 and 1.85 Å, respectively (Fig. 5). The adsorption energy,

Table 1: The adsorption energies of atomic Li and Li⁺ (E_{ad} , kcal/mol) on different nanoparticles.

| Nanoparticle | E_{ad} 6-31+G(d) | E_{ad} 6-31++G(d) | E_{ad} 6-31+G(d) Solvent* | E_{HOMO} | E_{LUMO} | E_g | % ΔE_g | ΔE_{cell} | V_{cell} |
|-----------------------|-----------------------|------------------------|--------------------------------|------------|------------|-------|----------------|--------------------|------------------|
| Sum | --- | --- | --- | -6.95 | -0.29 | 6.67 | --- | --- | --- |
| Sum/Li | -3.53 | -3.54 | -34.12 | -3.55 | -0.83 | 2.73 | -59.09 | --- | --- |
| Sum/Li ⁺ | -42.20 | -42.14 | -83.46 | -10.63 | -4.34 | 6.29 | -5.60 | -38.66 (-49.34) | -1.68 (-2.14) |
| Sum-i/Li | -10.77 | -10.77 | -32.44 | -3.47 | -0.83 | 2.64 | -60.37 | --- | --- |
| Sum-i/Li ⁺ | -44.55 | -44.47 | -82.51 | -10.94 | -4.57 | 6.37 | -4.48 | -33.78 (-50.07) | -1.46 (-2.17) |
| Cor | --- | --- | --- | -7.56 | -1.14 | 6.42 | --- | --- | --- |
| Cor/Li | -19.81 | -19.88 | -36.89 | -3.95 | -1.18 | 2.78 | -55.96 | --- | --- |
| Cor/Li ⁺ | -43.67 | -43.71 | -83.26 | -11.07 | -4.91 | 6.16 | -3.95 | -23.86 (-46.37) | -1.03 (-2.01) |
| Cor-i/Li | -22.24 | -22.19 | -34.44 | -3.95 | -1.18 | 2.78 | -56.75 | --- | --- |
| Cor-i/Li ⁺ | -43.25 | -43.20 | -83.57 | -11.45 | -5.06 | 6.39 | -0.38 | -21.02 (-49.13) | --- |
| Sheet | --- | --- | --- | -5.95 | -1.59 | 4.36 | --- | --- | --- |
| Sheet/Li | -17.14 | --- | --- | -3.48 | -1.49 | 1.99 | -54.34 | --- | --- |
| Sheet/Li ⁺ | -52.31 | --- | --- | -8.61 | -4.30 | 4.31 | -1.05 | -35.17 | --- |

Energies of HOMO, LUMO, and HOMO-LUMO gap (E_g) in eV. ΔE_g indicates the change of E_g of nanoparticles after the Li/Li⁺ adsorption. The total energy change (ΔE_{cell} , kcal/mol) and cell voltage (V) of the nanoparticles based Li-ion battery.

*Solvent is ethylene carbonate, EC, and the ΔE_{cell} and V_{cell} values in parenthesis are in the EC solvent.

**Fig. 3: Density of states (DOS) plot of Sum (right) and Li⁺- Sum complex (left).**

E_{ad} , of the Li⁺ ion inside the Sum-i is -44.55 kcal/mol that is larger than that of the Li neutral (-10.77 kcal/mol) (Table 1). These adsorption energies, E_{ad} , indicate a good interaction between Sum and Li⁺ ion as well as Li neutral inside the bowl of Sum-i respect to outside the bowl of Sum.

The LUMO level considerably stabilized from -0.29 eV in Sum-i to -4.57 eV in the Li⁺-Sum-i complex (Table 1), leading to slightly decrease in the E_g (~-4.5%). The changes in HOMO, LUMO and E_g are demonstrated in Fig. 6 by Density of State (DOS) diagrams.

The Li adsorption considerably makes the SOMO unstable due to being an unpaired electron in HOMO of the Li-Sum-i complex. This SOMO level is changed from -6.95 to -3.47 eV which is singly occupied. The energy of the LUMO level is almost slightly changed from -0.29 to -0.83 eV as shown in Table 1 and Fig. 6. As a result of large change in HOMO, the E_g is significantly narrowed by about 60.4%, indicating that the effect of Li adsorption on the E_g is much more than that of the Li⁺ adsorption process.

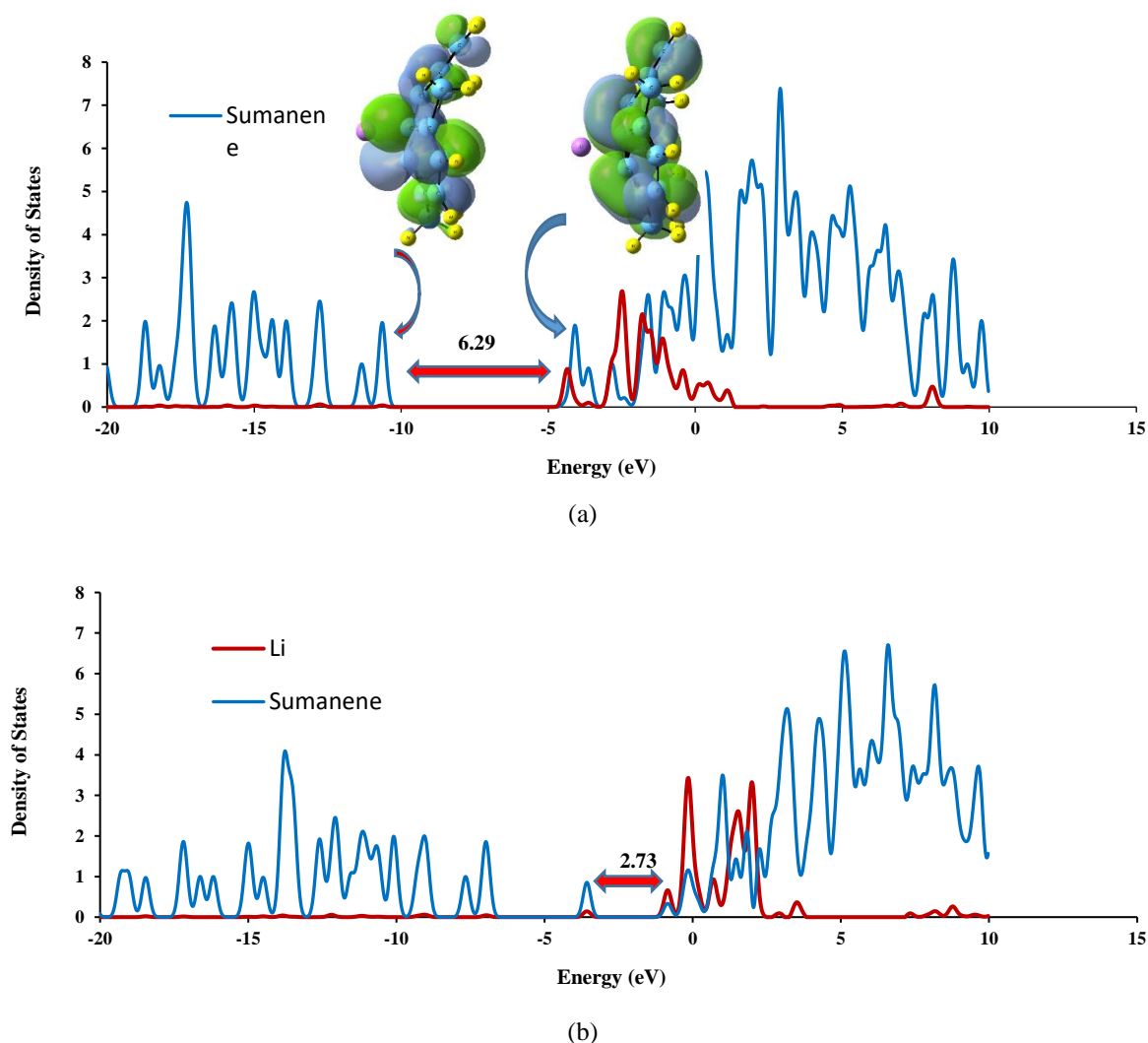


Fig. 4: Partial density of states (PDOS) plot of Li^+ -Sum and Li-Sum. (a) PDOS plot of Li^+ -Sum (b) PDOS plot of Li-Sum.

Adsorption of Li/Li⁺ outside the bowl of corannulene

Corannulene molecule consists of a cyclopentane ring fused with four benzene rings which is also known as a bucky bowl. Cor exhibits a bowl-to-bowl inversion with an inversion barrier of 10.2 kcal/mol at $-64\text{ }^\circ\text{C}$ [28]. During optimization, the Li^+ ion and Li atom were located above the plane of the five-membered ring of Cor with distances of 1.89 and 1.82 Å, respectively (Fig. 7). This indicates a good interaction between Cor and both Li^+ ion and Li neutral. The adsorption energy, E_{ad} , of the Li^+ ion on the Cor is -43.67 kcal/mol that is larger than that of the Li neutral (-19.81 kcal/mol) (Table 1). The interactions between Cor and both Li^+ ion and Li neutral are stronger than those of surname.

The LUMO level considerably stabilized from -1.14 eV in Cor to -4.91 eV in the Cor- Li^+ complex (Fig. 8 and Table 1), leading to slightly decrease in the E_g ($\sim -3.9\%$). The changes in HOMO, LUMO and E_g are demonstrated in Fig. 4 by density of state (DOS) diagrams. Plot of density of states, DOS, clearly indicates that a new level produced at the E_g gap of pristine mostly arises from Li^+ cation which leads to decrease slightly in E_g of the Li^+ -Cor complex (Fig. 8).

The effect of atomic Li adsorption on the electronic properties of Cor-Li is different from that of Cor- Li^+ . The Li adsorption considerably makes the SOMO unstable due to being an unpaired electron in HOMO of the Cor-Li complex. This SOMO level is changed from -7.56 to

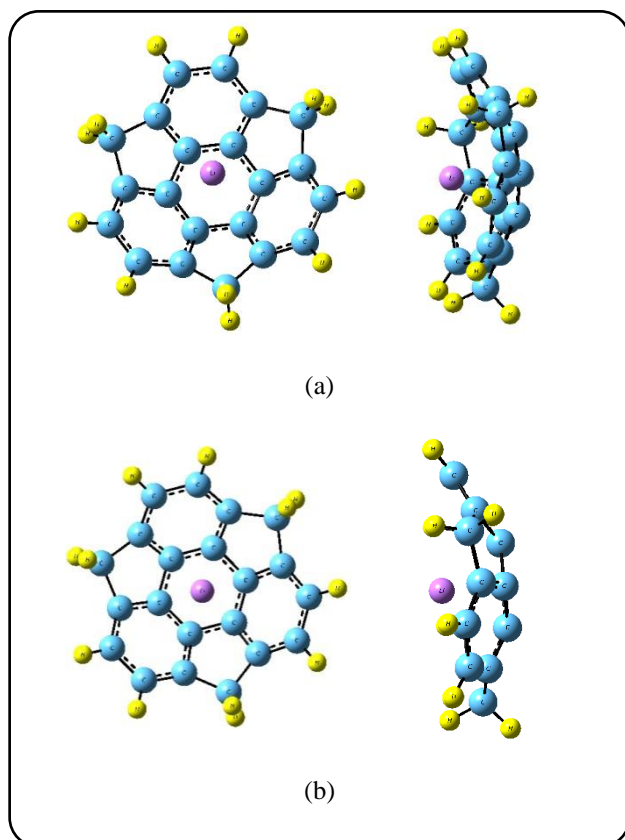


Fig. 5: Optimized structures of Li^+ and Li-Sum-i complexes. (a) $\text{Li}^+-\text{Sum-i}$ complex (b) Li-Sum-i complex, Distances are in Å.

-3.95 eV which is singly occupied. In a good agreement with the sharp energy change, the shape of HOMO is changed significantly by transferring to the adsorbing area. The energy of the LUMO level is unchanged as shown in Table 1 and Fig. 8. Large change in HOMO, the E_g is significantly decreased by 56.0%, indicating that the Li adsorption affects to the E_g much more than that of the Li^+ adsorption. The changes in HOMO, LUMO and E_g are illustrated in Fig. 8 using density of state (DOS) diagrams.

Adsorption of Li/Li^+ inside the bowl of corannulene

The distances of Li^+ ion and Li atom inside the plane of the five-membered ring of Cor are 1.92 and 1.84 Å, respectively (Fig. 9). The adsorption energy, E_{ad} , of the Li^+ ion inside the Cor is -43.25 kcal/mol that is larger than that of the Li neutral (-22.24 kcal/mol) (Table 1).

The LUMO level considerably stabilized from -1.14 eV in Cor to -5.06 eV in the $\text{Li}^+-\text{Cor-i}$ complex (Table 1); leading to slightly decrease in the E_g (~-0.4%). The changes in HOMO, LUMO and E_g are demonstrated in Fig. 10 by density of state (DOS) diagrams.

The Li adsorption inside the bowl of Cor considerably makes the SOMO unstable due to being an unpaired electron in HOMO of the Li-Cor-i complex. This SOMO level is changed from -7.56 to -3.95 eV which is singly occupied. The energy of the LUMO level is almost slightly changed from -1.14 to -1.18 eV as shown in Table 1 and Fig. 10. As a result of large change in HOMO, the E_g is significantly narrowed by about -56.75%, indicating that the effect of Li adsorption on the E_g is much more than that of the Li^+ adsorption process.

Adsorption of Li/Li^+ over nanosheet

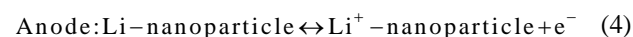
The adsorption energy, E_{ad} , of the Li^+ ion on the nanosheet is -52.3 kcal mol⁻¹ that is larger than that of the Li neutral (-17.14 kcal mol⁻¹) (Fig. 11 and Table 1).

The LUMO level considerably stabilized from -1.59 eV in nanosheet to -4.30 eV in the nanosheet- Li^+ complex (Fig. 12 and Table 1), leading to slightly decrease in the E_g (~-1.05%). The changes in HOMO, LUMO and E_g are demonstrated in Fig. 12 by Density of State (DOS) diagrams.

The Li adsorption considerably makes the SOMO unstable due to being an unpaired electron in HOMO of the nanosheet-Li complex. This SOMO level is changed from -5.95 to -3.48 eV which is singly occupied. The energy of the LUMO level is slightly changed as shown in Table 1 and Fig. 1. Large change in HOMO, the E_g is significantly decreased by 54.3%, indicating that the Li adsorption affects to the E_g much more than that of the Li^+ adsorption. The changes in HOMO, LUMO and E_g are illustrated in Fig. 12 using Density of State (DOS) diagrams.

Comparison the nanoparticles in the Li^+ -ion batteries (LIBs)

Three types of nanoparticles suggested as an anode for the LIBs. The formal reactions in the anode and cathode are the following [29]:



This reaction can be divided into several formal reactions that are presented below:



The total reaction of the cell can be defined as:

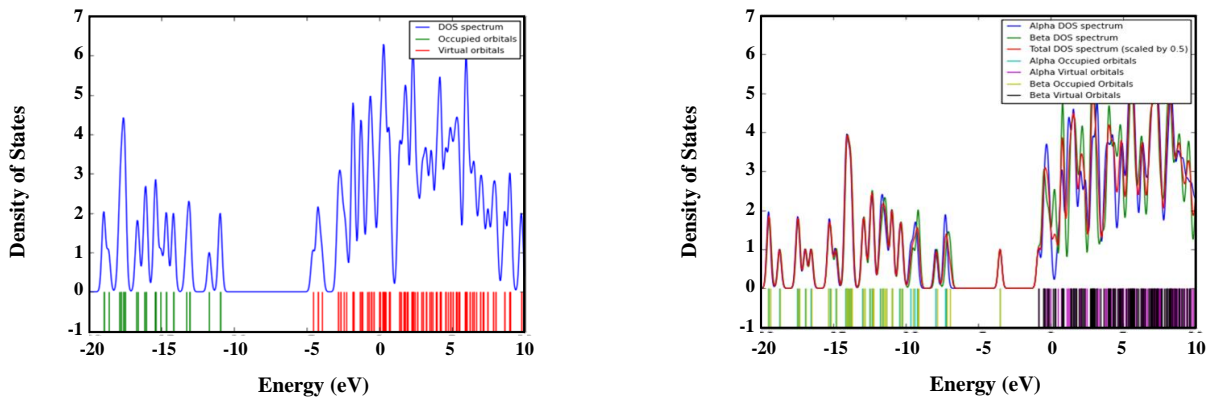


Fig. 6. Density of states (DOS) plot of (a) Li^+ -Sum-I; (b) Li -Sum-i.

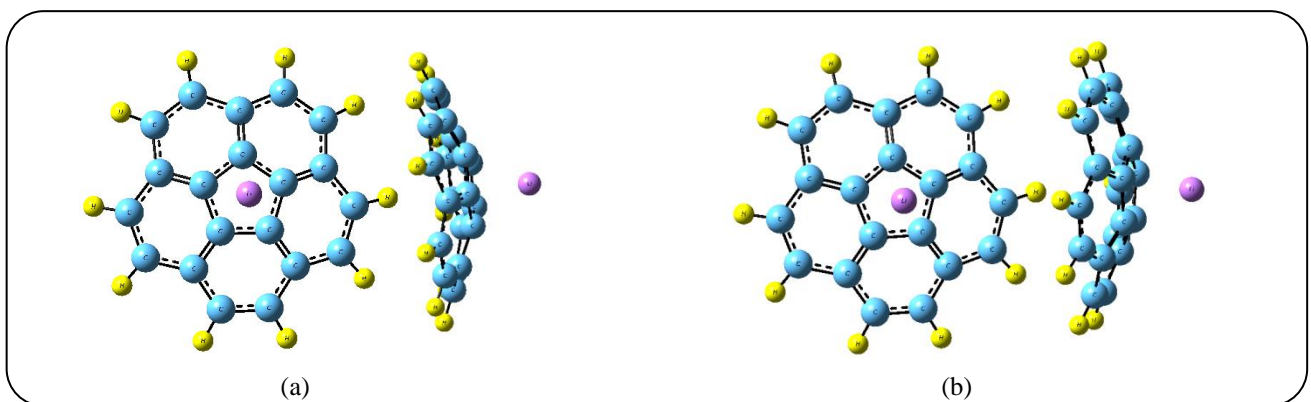


Fig. 7: Optimized structures of Li^+ and Li -Cor complexes. (a) Li^+ -Cor complex (b) Li -Cor complex, Distances are in Å.

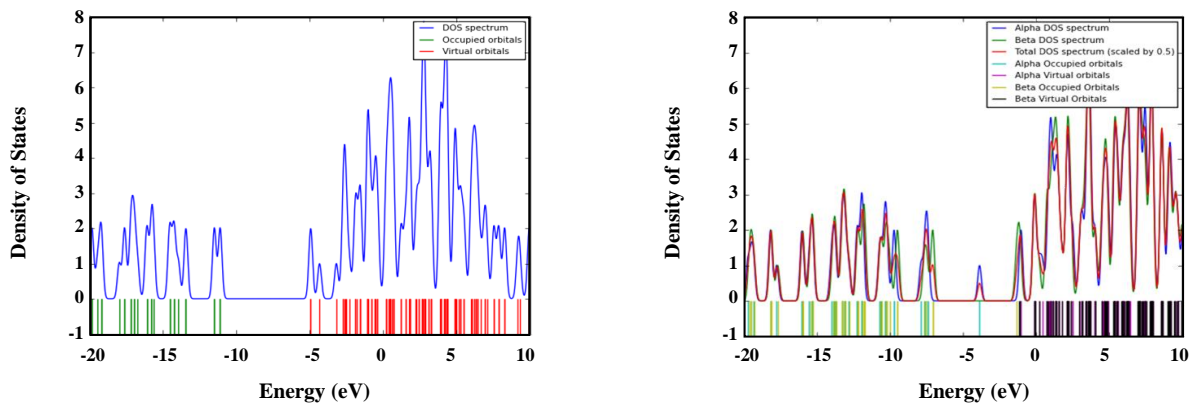
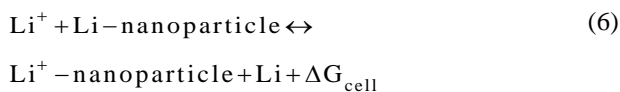
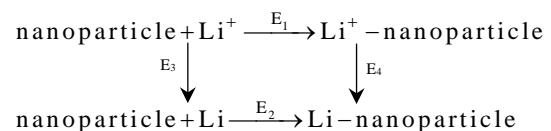


Fig. 8: Density of states (DOS) plot of (a) Li^+ -Cor; (b) Li -Cor.



This equation is related to the binding energy in one hand and to the ionization potential of Li on the other hand.



where, E_1 and E_2 are binding energies and E_3 and E_4 are ionization potential which can be related with

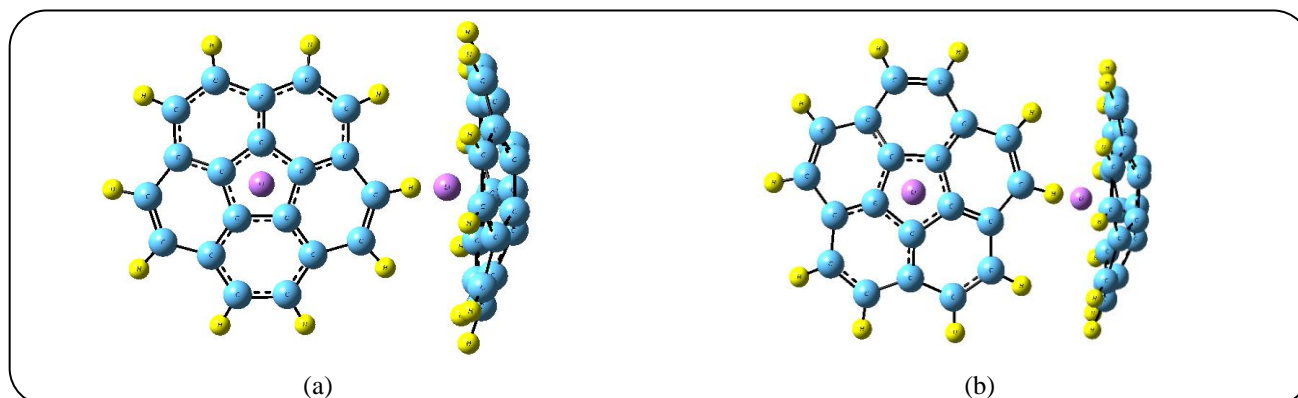


Fig. 9: Optimized structures of Li^+ and Li-Cor-i complexes. (a) Li^+ -Cor-i complex (b) Li-Cor-i complex, Distances are in Å.

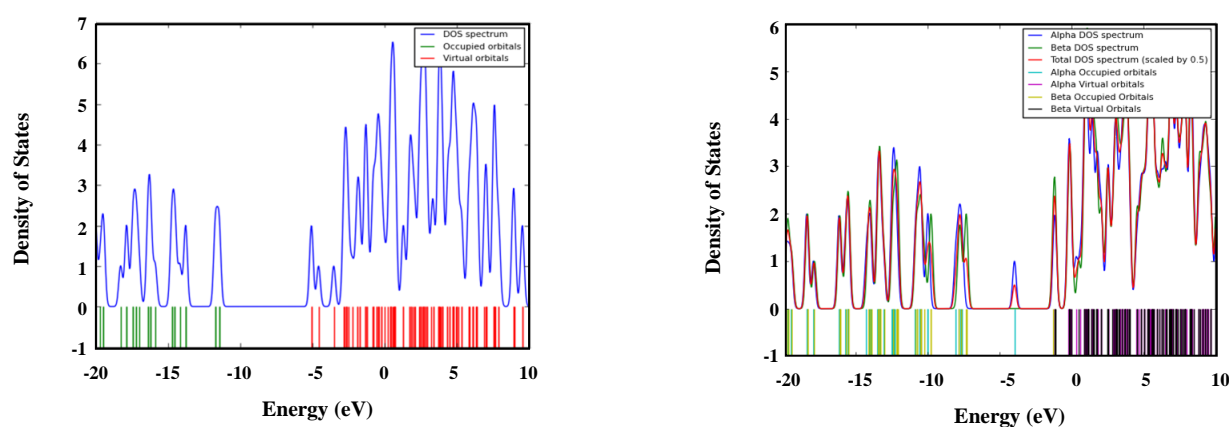


Fig. 10: Density of states (DOS) plot of (a) Li^+ -Cor-i; (b) Li-Cor-i.

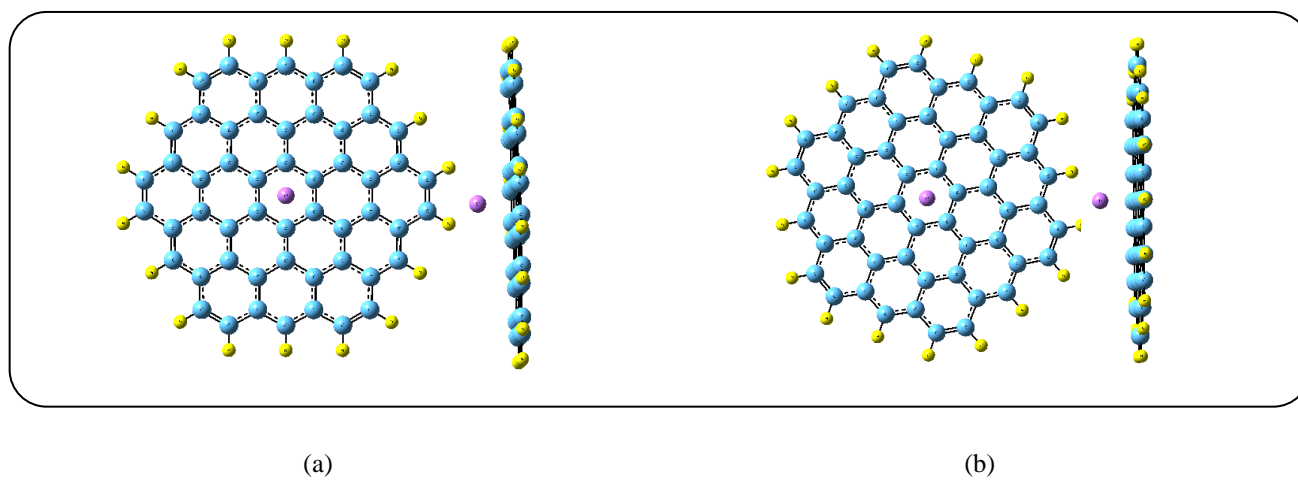


Fig. 11: Optimized structures of Li^+ and Li-Sheet complexes. (a) Li^+ -Sheet complex (b) Li-Sheet complex, Distances are in Å.

the following equation: $E_1 + E_4 = E_3 + E_2$ or $E_1 - E_2 = E_3 - E_4$

The Nernst equation is used to obtain the cell voltage (V_{cell}) as follows:

$$V_{\text{cell}} = -\Delta G_{\text{cell}} / zF \quad (7)$$

$V_{\text{cell}} = -\Delta G_{\text{cell}}/zF$ where, F and z are the Faraday constant (96500 C/mol) and charge of Li^+ ($z=2$, the cation

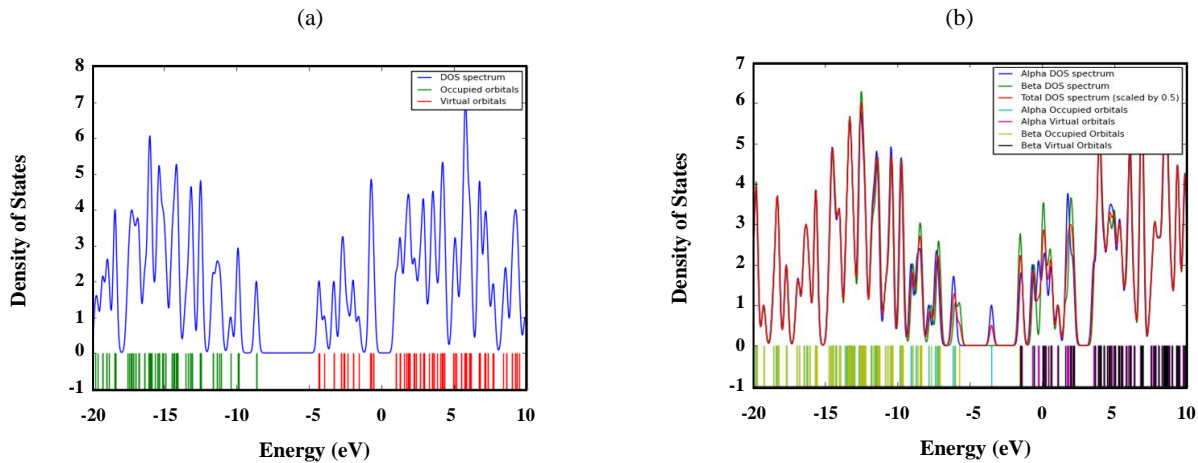


Fig. 12: Density of states (DOS) plot of (a) Li^+ -Sheet; (b) Li -Sheet.

in electrolyte), respectively. The ΔG_{cell} is the Gibbs free energy difference of the total reaction of cell. For DFT calculations at 0 K, it can be presented:

$$\Delta G_{\text{cell}} = \Delta E_{\text{cell}} + P\Delta V - T\Delta S \quad (8)$$

In previous reports we confirm that the amount of volume and entropy contribution are very small (< 0.01 V) to the V_{cell} [29]. Therefore, the V_{cell} for Li^+ - or Li -nanoparticle can be determined by calculating the internal energy change (ΔE) from Eqs. 6 and 8 as follows:

$$\Delta E_{\text{cell}} \sim \Delta G_{\text{cell}} = E_{\text{Li}^+} + E_{\text{Li}^+-\text{nanoparticle}} - E_{\text{Li}^+} - E_{\text{Li-nanoparticle}} \quad (9)$$

Eq. (9) indicates that the simultaneous strong interaction between Li^+ and nanoparticle and weak interaction between Li atom and nanoparticle obtain more negative and high ΔE_{cell} . In conclusion, the strong adsorption of Li^+ and weak adsorption of Li on the nanoparticle lead to high V_{cell} (Table 1). The adsorption energy between Li^+ and nanoparticles, E_{ad} , is increased in the order: Sheet $>$ Sum-i $>$ Cor $>$ Cor-i $>$ Sum. The ΔE_{cell} , and V_{cell} are calculated for three nanoparticles which presented in Table 1 and schemed in Fig. 13. The ΔE_{cell} , and V_{cell} values for three nanoparticles in LIBs changed in the same order: Sum $>$ Sheet $>$ Sum-i $>$ Cor $>$ Cor-i. The largest ΔE_{cell} and V_{cell} values are -38.66 kcal/mol and 1.68 V, respectively, which related to Sum. Despite to the highest interaction between Li^+ and nanosheet, the ΔE_{cell} and V_{cell} for LIBs-nanosheet are -35.17 kcal/mol and 1.53 V, respectively, which are lower than the values of Sum.

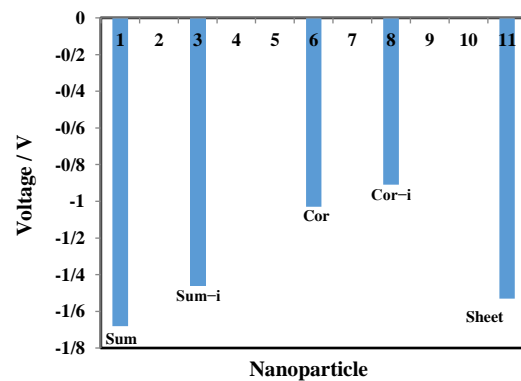


Fig. 13: The diagram of the cell voltage vs. different nanoparticles as an anode of Li ion batteries, LIBs.

The V_{cell} for Sum is the highest because the interaction between Sum and the Li neutral is the lowest. The calculated V_{cell} for LIBs-Sum is higher than 1.45 V for Li-ion battery which reported for nanotube by Gao *et al.* [30]. The strong interaction between Li^+ and nanoparticle leads to higher V_{cell} amount of the LIBs-nanoparticle while the weak interaction between the Li atom and nanoparticle leads to higher the V_{cell} value. The lowest V_{cell} value belongs to the LIBs-Cor-i due to highest interaction between the Li neutral and Cor-i. In general, the V_{cell} value for LIBs-nanoparticles are from -0.9 to -1.7 V, makes these nanoparticles the promising candidates which could apply to manufacture of the LIBs as anode. We can conclude that in the study nanoparticles, the interaction between the Li neutral and nanoparticles play a significant role in V_{cell} respect to the interaction between the Li^+ neutral and nanoparticles.

The Sum and Cor nanoparticles were optimized using 6-31++G (d,p) basis set due to comparison with 6-31+G (d,p) results. The calculations indicate that the data obtained by 6-31++G(d,p) basis set are very similar to 6-31+G(d,p) basis set showing an additional diffusion parameter does not affect the results. Meanwhile, DFT calculations on the Sum-Li⁺/Li and Cor-Li⁺/Li complexes in presence of an electrolyte solvent, ethylene carbonate, EC, gave interesting results. The EC has a high dielectric constant of 95.3 which led to significant effect on V_{cell} results (Table 1). The adsorption energies as well as V_{cell} increased when EC solvent was used. It is seemed that V_{cell} for Sum-i and Cor-i are more than Sum and Cor, respectively maybe due to solvation effects of Sum and Cor which is in contract to gas phase.

CONCLUSIONS

In this work, the adsorption of Li⁺ and Li over three types of the nanoparticles including sumanene (Sum), corannulene (Cor) and nanosheet was studied to scrutinize their possible application as an anode of LIBs. The interaction between Li⁺ and the surface of nanoparticles is clearly stronger than that of the Li which clarifies that these nanoparticles are appropriate as an anode of LIBs.

The energy adsorption, E_{ad} , between Li⁺ and nanosheet was the highest adsorption energy which E_{ad} were changed in the order: Sheet > Sum-i > Cor > Cor-i > Sum. However, the cell voltage, V_{cell} , was the highest for sumanene. The changes in V_{cell} of LIBs are in the order: Sum > Sheet > Sum-i > Cor > Cor-i. The interaction between Li⁺ and Li and nanoparticles play a remarkable role in determination of the cell voltage. The strong interaction between Li⁺ and nanoparticles and weak interaction between Li and nanoparticles led to obtain a high V_{cell} .

Received : Apr. 29, 2019 ; Accepted : Sep. 2, 2019

REFERENCES

- [1] a) Danuta H., Juliusz U., [Electric Dry Cells and Storage Batteries](#), US Patent 3,043,896, 1962;
b) Xu W., Wang J., Ding F., Chen X., Nasybulin E., Zhang Y. and Zhang J.-G. [Lithium Metal Anodes for Rechargeable Batteries](#), *Energy Environ. Sci.*, **7**: 513–537 (2014).
- [2] Siadati S.A., Vessally E., Hosseinian A., Edjlali L., [A Density Functional Theory Study on the Interaction Between 5-Fluorouracil Drug and C24 Fullerene](#). *Synthetic Met.* **220**: 606–611 (2016).
- [3] Siadati S.A., Vessally E., Hosseinian A., Edjlali L., [Selective Sensing of Ozone and the Chemically Active Gaseous Species of the Troposphere by Using the C20 Fullerene and Graphene Segment](#), *Talanta*, **162**: 505–510 (2017).
- [4] Vessally E., Soleimani-Amiri S., Hosseinian A., Edjlali L., Bekhradnia A., [Selective detection of cyanogen halides by BN Nanocluster](#) *Physica E, J. Alloys Compd.*, **87**: 308–311 (2017).
- [5] Hosseinian A., Saedi Khosroshahi E., Nejadi K., Edjlali E., Vessally E., [A DFT Study on Graphene, SiC, BN, and AlN Nanosheets as Anodes in Na-Ion Batteries](#). *Mol. Model.*, **23**: 354 (2017).
- [6] Nejadi K., Hosseinian A., Edjlali L., Vessally E., [The Effect of Structural Curvature on the Cell Voltage of BN Nanotube Based Na-Ion Batteries](#), *J. Mol. Liq.*, **229**: 167–171 (2017).
- [7] Subalakshmi P., Sivashanmugam A., [CuO Nano Hexagons, an Efficient Energy Storage Material for Li-Ion Battery Application](#), *J. Alloys Compd.*, **690**: 523–531 (2017).
- [8] Nejadi K., Hosseinian A., Bekhradnia A., Vessally E., Edjlali L., [Selective Detection of Cyanogen Halides by BN Nanocluster](#), *J. Mol. Graph. Model.*, **74**: 1–7 (2017).
- [9] Jing Y., Zhou Z., Cabrera C.R., Chen Z.F., [Graphene, Inorganic Graphene Analogs and their Composites for Lithium Ion Batteries](#), *J. Mater. Chem. A*, **2**: 12104–12122 (2014).
- [10] Hao J.Y., Zheng J.F., Ling F.L., Chen Y.K., Jing H. R., Zhou T.W., Fang L., Zhou M., [Strain-engineered Two-Dimensional MoS2 as Anode Material for Performance Enhancement of Li/Na-Ion Batteries](#), *Sci. Rep.* **8**: 2079-2079 (2018).
- [11] Li W., Yang Y.M., Gang Z., Zhang Y.W., [Ultrafast and Directional Diffusion of Lithium in Phosphorene for High-Performance Lithium-Ion Battery](#), *Nano Lett.*, **15**: 1691–1697 (2015).
- [12] Wang D.S., Gao Y., Liu Y.H., Jin D., Gogotsi Y., Meng X., Du F., Chen G., Wei Y.J., [First-Principles calculations of Ti2N and Ti2NT2 \(T = O, F, OH\) Monolayers as Potential Anode Materials for Lithium-Ion Batteries and Beyond](#), *J. Phys. Chem. C*, **121**: 13025–13034 (2017).

- [13] Kim S.K., Chang H., Kim C.M., Yoo H., Kim H., Jang H.D., Fabrication of Ternary Silicon–Carbon Nanotubes–Graphene Composites by Co–Assembly in Evaporating Droplets for Enhanced Electrochemical Energy Storage, *J. Alloys Compd.* **751**: 43–48 (2018).
- [14] Chen S., Hassanzadeh-Aghdam M.K., Ansari R., An Analytical Model for Elastic Modulus Calculation of SiC Whisker-Reinforced Hybrid Metal Matrix Nanocomposite Containing SiC Nanoparticles, *J. Alloy. Compd.*, **767**: 632-641 (2018).
- [15] Guo H., Qian K., Cai A., Tang J. Liu J., Ordered gold Nanoparticle Arrays on the Tip of Silver Wrinkled Structures for Single Molecule Detection, *Sensor. Actuat B-Chem.*, **300**: 126846, (2019).
- [16] Liu Y., Zhang Q., Xu M., Yuan H., Chen Y., Zhang J., Luo K., Zhang J., You B., Novel and Efficient Synthesis of Ag-ZnO Nanoparticles for the Sunlight-Induced Photocatalytic Degradation, *Appl. Surf. Sci.*, **476**: 632-640 (2019).
- [17] Wang X., Wang J., Sun X., Wei S., Cui L., Yang W., Liu J., Hierarchical coral-like NiMoS Nano hybrids as Highly Efficient Bifunctional Electrocatalyst for Overall urea Electrolysis, *Nano Res.*, **11**: 988–996 (2018).
- [18] Wang M., Yang L., Hu B., Liu J., He L., Jia Q., Song Y., Zhang Z., Bimetallic NiFe Oxide Structures Derived from Hollow NiFe Prussian Blue Nanobox for Label-Free Electrochemical Biosensing Adenosine Triphosphate, *Biosens. Bioelectron.*, **113**: 16-24 (2018).
- [19] Wang Y., Yao M., Ma R., Yuan Q., Yang D., Cui B., Ma C., Liu M., Hu D., Design strategy of Barium Titanate/Polyvinylidene Fluoride-Based Nanocomposite Films for High Energy Storage, (2020). <https://doi.org/10.1039/C9TA11527G>
- [20] Sakurai H., Daiko T., Hirao T., A Synthesis of Sumanene, a Fullerene Fragment, *Science*, **301**: 1878–1878 (2003)
- [21] Barth W.E., Lawton R.G., Dibenzo[ghi,mno]fluoranthene, *J. Am. Chem. Soc.* **88**(2): 380–381 (1966).
- [22] Lawton, R.G., Barth W.E.. Synthesis of Corannulene. *J. Am. Chem. Soc.* **93**(7): 1730–1745 (1971).
- [23] Chai J.-D., Head-Gordon M. Long-Range Corrected Hybrid Density Functionals with Damped Atom–Atom Dispersion Corrections., *Phys. Chem. Chem. Phys.*, **10**: 6615 (2008).
- [24] Frisch M.J., Trucks G.W., Schlegel H.B., Scuseria G.E., Robb M.A., cheeseman J.R., Zakrzewski V.G., Montgomery J.A., Stratmann J.R.E., Burant J.C., Dapprich S., Millam J.M., Daniels A.D., Kudin K.N., Strain M.C., Farkas O., Tomasi J.V., Barone, Cossi M., Cammi R., Mennucci B., Pomelli C., Adamo C., Clifford S., Ochterski J., Petersson G.A., Ayala P.Y., Cui Q., Morokuma K., Malick D.K., Rabuck A.D., Raghavachari K., Foresman J.B., Cioslowski J., Ortiz J.V., Baboul A.G., Stefanov B.B., Liu G., Liashenko A., Piskorz P., Komaromi I., Gomperts R., Martin R.L., Fox D.J., Keith T., Al-Laham M.A., Peng C.Y., Nanayakkara A., Gonzalez C., Challacombe M., Gill P.M.W., Johnson B., Chen W., Wong M.W., Andres J.L., Gonzalez C., Nead-Gordon M., Replogle E.S., Pople J.A., , Gaussian 98, Revision A.7, Gaussian, Inc., Pittsburgh PA., (2009).
- [25] Boys S.F., Bernardi F., The Calculation of Small Molecular Interactions by the Differences of Separate Total Energies. Some Procedures with Reduced Errors, *Mol. Phys.*, **19**: 553–561 (1970).
- [26] O’Boyle N., Tenderholt A., Langner K., A library for package-Independent Computational Chemistry Algorithms *J. Comput. Chem.*, **29**: 839–845 (2018).
- [27] Hidehiro S., Taro D., Hiroyuki S., Toru A., Toshikazu H., Structural Elucidation of Sumanene and Generation of Its Benzylic Anions, *J. Am. Chem. Soc.*, **127**: 11580 –11581, (2005).
- [28] Scott, L. T.; Hashemi, M. M.; Bratcher, M. S.. Corannulene Bowl-to-Bowl Inversion is Rapid at Room Temperature, *J. Am. Chem. Soc.*, **114**(5): 1920–1921 (1992).
- [29] Denis P. A., Iribarne F. Alkali Metal Mediated C–C Bond Coupling Reaction, *Chem. Phys. Lett.*, **573**: 15–18 (2013).
- [30] Gao Z., Chin C.S., Chiew J.H.K., Zhang J.J.C., Nonlinear Temperature-Dependent State Model of Cylindrical LiFePO₄ Battery for Open-Circuit Voltage, Terminal Voltage and State-of-Charge Estimation with Extended Kalman Filter, *Energy*, **10**: 1503 (2017).